

ModaNet: A Large-Scale Street Fashion Dataset with Polygon Annotations

Shuai Zheng

eBay

San Jose, California

shuzheng@ebay.com

M. Hadi Kiapour

eBay

San Francisco, California

mkiapour@ebay.com

Fan Yang

eBay

San Jose, California

fyang4@ebay.com

Robinson Piramuthu

eBay

San Francisco, California

rpiramuthu@ebay.com

ABSTRACT

Understanding clothes from a single image has strong commercial and cultural impacts on modern societies. However, this task remains a challenging computer vision problem due to wide variations in the appearance, style, brand and layering of clothing items. We present a new database called “ModaNet”, a large-scale collection of images based on Paperdoll dataset [40]. Our dataset provides 55,176 street images, fully annotated with polygons on top of the 1 million weakly annotated street images in Paperdoll. ModaNet aims to provide a technical benchmark to fairly evaluate the progress of applying the latest computer vision techniques that rely on large data for fashion understanding. The rich annotation of the dataset allows to measure the performance of state-of-the-art algorithms for object detection, semantic segmentation and polygon prediction on street fashion images in detail.

CCS CONCEPTS

- Computing methodologies → Artificial intelligence; Computer vision; Computer vision problems; Image segmentation; Object detection;

KEYWORDS

Fashion, Computer Vision, Dataset

ACM Reference Format:

Shuai Zheng, Fan Yang, M. Hadi Kiapour, and Robinson Piramuthu. 2018. ModaNet: A Large-Scale Street Fashion Dataset with Polygon Annotations. In *Proceedings of ACM Multimedia conference (ACM Multimedia’18)*, Jennifer B. Sartor, Theo D’Hondt, and Wolfgang De Meuter (Eds.). ACM, New York, NY, USA, 9 pages. <https://doi.org/10.1145/nnnnnnnnnnnnnn>

1 INTRODUCTION

Fashion understanding and analysis have been a popular topic in computer vision community for several years. With abundant visual information available, fashion is a natural domain to apply various

Permission to make digital or hard copies of part or all of this work for personal or classroom use is granted without fee provided that copies are not made or distributed for profit or commercial advantage and that copies bear this notice and the full citation on the first page. Copyrights for third-party components of this work must be honored. For all other uses, contact the owner/author(s).

ACM Multimedia’18, 22 - 26 October 2018, Seoul, Korea

© 2018 Copyright held by the owner/author(s).

ACM ISBN 978-x-xxxx-xxxx-x/YY/MM.

<https://doi.org/10.1145/nnnnnnnnnnnnnn>

computer vision techniques to improve online shopping experience and create significant business value. Due to the enormous variety of clothing types and unpredictable clothing appearance, understanding fashion even in a single image remains an open problem. Apart from identifying garments from a large number of categories and differentiating abstract styles from each other, which are already difficult, tasks such as localizing and segmenting fashion items are more desirable for real-life applications, including online shopping, personalized recommendation, and virtual try-on, *etc.* For example, given a street photo containing a celebrity, a shopper might be particularly interested in a specific fashion item, such as the pair of shoes the celebrity wears, and exploring more choices of the same style, shape or color. In this case, the shoes may only occupy a small portion of the entire photo, while the majority of the photo is not relevant to this shopper’s intent. Therefore, it is important to automatically localize and segment the shoes rather than sending the entire image to a visual search engine that may return irrelevant results. By analyzing individual fashion items separately and the relationship between them, we move towards understanding the outfit as a whole. In this context, automatic detection and segmentation is even more challenging as it requires more granular annotations for garment layers rather than image-level labels only, as well as other complications introduced by difficult body pose and clothing deformation.

To address the above-mentioned problems, the first step is to have a high-quality, large-scale dataset that is the foundation of training good models. Such fine-grained annotations are usually expensive to acquire as they require numerous human resources and domain knowledge compared to generating image-level labels. Previous works [26, 40, 41] propose several datasets with pixel-level annotations for fashion parsing, but their annotated sets are limited to thousands of images only. Moreover, these datasets mainly focus on street fashion images containing people in the frontal pose without many pose variations, hence the trained model may only work well in limited scenarios. Recently, Liu *et al.* propose a large-scale dataset called DeepFashion. Apart from image-level labels specifying the type of clothes, the DeepFashion dataset also contains richer information such as binary attributes and landmarks that are useful to improve clothes retrieval performance. Although attributes and landmarks provide certain lower level information, they are still too coarse to train a good model to localize and segment individual fashion items.

In this work, we introduce a new fashion dataset called ModaNet consisting of 55,176 high-quality, fully-annotated street fashion images on top of the 1 million weakly labeled images in the Paper-doll dataset [40]. For the images that are fully-annotated, we have obtained pixel-level segmentation masks and polygons enclosing individual fashion items. We annotate 13 categories that are of the most interest in research and real-world commerce applications. Compared to its precedents, the ModaNet dataset has the following improvements. First, our ModaNet dataset is 10× larger compared to other fashion datasets with pixel-level annotations, thus providing more data to train a better model specialized in detection and segmentation. Second, the annotated images are carefully selected to ensure diversity in human poses, *i.e.*, not limited to the frontal view. In this way, training on this data grants a more generalizable model. Third, not only we provide pixel-level segmentation masks, but we also release coordinates of polygons enclosing individual fashion items. The polygons record the shape information of object boundary and serve as an alternative way to segment objects. Rectangular bounding box annotations are inferred from polygons to enable fashion item detection.

With fine-grained pixel-level masks, polygons and bounding boxes, we conduct various experiments to demonstrate the usefulness of the ModaNet dataset. Specifically, we investigate and compare the performance of several state-of-the-art deep neural networks for detection and semantic segmentation on this dataset, along with in-depth analysis and discussions. Additionally, we train a network to perform polygon prediction and verify its capability of capturing the boundary of objects, posing a potential research direction for fashion item understanding. From extensive experimental validation, we show that the proposed dataset enables multiple tasks to achieve promising results, which are difficult to obtain from small-scale and weakly annotated datasets.

2 RELATED WORK

2.1 Datasets

Numerous datasets specifically tailored for fashion have been introduced and contributed to the advancement of various vision algorithms. Some datasets contain only a particular fashion category, such as the UT Zappos50K dataset [43], while some include more types of fashion items [17, 18]. Complementary information like attributes and landmarks are also provided in some datasets for more fine-grained analysis. These datasets are mostly designed for image retrieval where the task is to match similar clothes, thus often consist of a large number of images from different domains such street fashion, and product photos. For example, a recent DeepFashion dataset contains as many as 800,000 images [30].

On the other hand, some datasets aim at parsing individual fashion items given a street photo image [20, 26, 40–42]. Different from the datasets used for image retrieval that only have image-level labels, these datasets have pixel-level annotations for each type of category, which can be used as segmentation masks to train segmentation models. Although annotations are richer, these datasets usually contain only hundreds or thousands of images due to the difficulty of acquiring pixel-level annotations. Therefore, although they are useful for identifying fashion items more accurately, they are not especially helpful for real-world applications, where the

diversity of fashion items is enormous regarding type, appearance, composition, and style, *etc.*

In contrast to the afore-mentioned datasets, our ModaNet dataset advances the quality of data regarding both scale and granularity of annotations. We have more than 55,000 fully-annotated images with pixel-level segments, polygons and bounding boxes covering 13 categories. A comparison is shown in Table 1.

2.2 Detection

There are various applications based on existing datasets that try to understand fashion from different perspectives. One important task is to detect fashion items from images. Recently, various approaches based on deep neural networks have been proposed for generic object detection and achieved promising results, among which, some representative works are RCNN [12], Fast RCNN [11], Faster RCNN [32], SSD [28], R-FCN [7], YOLO [31], *etc.* To improve the performance of these detectors, several modifications have been proposed. Shrivastava *et al.* [36] propose to use online hard negative mining to adaptively select diverse, high-loss samples for training. Lin *et al.* [24] propose the focal loss as an alternative way to do hard negative mining to alleviate the effect of overwhelming negative samples. Bodla *et al.* [2] introduce a soft-NMS to replace the traditional non-maximal suppression (NMS) used in object detection to discount the confidence score of predicted boxes rather than completely discarding them. By changing the backbone networks used in the detector, feature pyramid network [23], also called RetinaNet, has improved the detection accuracy, where feature maps from different convolutional layers are fused to provide more discriminative power. Deformable convolutional networks [8] also greatly improves detection performance for non-rigid objects by allowing convolution to operate on irregular regions instead of a grid.

Regarding fashion item detection specifically, Hara *et al.* [13] incorporate contextual information from body poses to guide detection and extract features from an off-the-shelf deep neural network. Liu *et al.* [30] present preliminary results using Fast RCNN trained on the DeepFashion dataset, but the model can only detect upper-body, lower-body and full-body objects due to the lack of fine-grained annotations.

2.3 Segmentation

The main focus of semantic image segmentation is to assign an object label to each pixel in an image. Recently, researchers have also begun tackling new problems such as instance segmentation [14], which aims to assign a unique identifier and a semantic meaningful label to each segmented object in the image. Semantic segmentation has traditionally been approached using probabilistic models known as Conditional Random Fields (CRFs) [16], which explicitly model the correlations among the pixels being predicted. However, in the recent years, learning a better discriminative feature representation [19, 35] has shown to play an important role in pushing the state-of-the-art performance of semantic image segmentation. The rise of deep Convolutional Neural Networks has significantly improved the way of learning feature representation. In particularly, the fully convolutional networks (FCNs) have shown significantly performance boost in semantic image segmentation [34].

There are two directions of improving semantic image segmentation. One is to improve the architectures or the bottleneck module of neural networks. The representative work is Chen *et al.* [4], which has further developed the FCNs using atrous layers. It has also used densely-connected CRFs as a post-processing step. Yu *et al.* [44] has improved semantic image segmentation by introducing dilated convolution, which increases the resolution of output feature maps without reducing the receptive field of individual neurons. Zhao [45] has proposed a pyramid scene parsing network that explores the prior global representation to produce good results on scene parsing task. Chen [5] has developed modules that employ the atrous convolution in cascade or in parallel to capture multi-scale context by adopting multiple atrous rates, which has shown state-of-the-art performance in PASCAL VOC benchmark. The other direction is to incorporate CRFs into an end-to-end trainable framework for semantic image segmentation, with the hope that joint training would help improve performance further. Zheng *et al.* [46] formulate an end-to-end trainable framework using the fully convolutional neural networks and densely-connected CRFs, while Liu *et al.* [29], Schwing *et al.* [33] and Lin *et al.* [22] have explored similar ideas along this line. These approaches are developed for generic object categories, and some are developed for scene parsing. Different from generic objects or scenes, there are more self-occlusion in fashion images. One goal of the ModaNet is to facilitate future semantic image segmentation that would perform well in fashion.

Several works have also explored semantic image segmentation in the context of fashion. Yamaguchi *et al.* [41] has pioneered the work in clothing parsing, and later further improved the fashion parsing performance by using retrieval-based approach [40]. Dong *et al.* [10] use Parselets as the building blocks of the parsing model. Liu *et al.* [27] present a solution that harnesses the context in fashion videos to boost the fashion parsing performance. Liang *et al.* [21] developed a convolutional neural network approach for human parsing. These works can be categorized into human parsing and clothing parsing. Clothing parsing attempts to identify the fine-grained categories of clothing items such as t-shirt and blouse, whereas human parsing tries to identify the body parts and broad clothing categories. The ModaNet dataset focuses on the clothing fashion parsing rather than human parsing.

3 THE MODANET DATASET

3.1 Constructing ModaNet

In this section, we explain the process of constructing the ModaNet dataset.

First, we collect 1 million images from the PaperDoll dataset [40], which are not fully annotated for object detection and semantic image segmentation purpose. This dataset has a large variety of images that are relevant to many fashion applications including street-to-shop and the shop-the-look.

Second, we apply Faster RCNN [32] that is pretrained on COCO dataset [25] to detect if there is only one person present in the image, and only collect those images with a single person. While addressing the images containing multiple persons is significantly more challenging due to occlusion and scale variance, we leave it in our future work and focus on dealing with the images containing only one person in the first release.

Among the initial set of selected images, we further manually select 2,000 images that are not suitable for annotations due to low image quality and 2,000 images that are high quality for annotation. On these 4,000 images, we fine-tune the last layer of a ResNet-50 [15] model pre-trained on ImageNet [9] as a classifier for image quality. We apply this classifier to the entire set of initially selected images to classify them into different levels of quality, and select those images of high quality and containing only one person. This step is necessary to reduce the number of images of the bad quality that are later sent to human annotators.

Finally, we send these images to human annotators. The tasks for human annotators are two-fold: one is to skip images they think is ambiguous to annotate, and the other one is to provide polygon annotations for individual objects in the image and assign a label from a pre-defined set of fashion object categories. We annotated this dataset through a collaboration with data annotation organization. We have 17 annotators (9 female, and 8 male) who were trained for 2 weeks before starting annotating. After training, all the annotators reached 99.5% internal quality accuracy, which was manually rated by 2 supervisors with computer vision background. The project was monitored daily. During the training phase, some annotators annotated images that were too blurry or dark, while other annotators annotated images containing no person or only the feet. We have fixed these issues by providing various sample images that they should skip or annotate. With polygon annotations, we can generate the ground truth for multiple computer vision tasks including object detection and semantic image segmentation.

3.2 Statistics

The dataset contains meta 13 categories, where each meta category groups highly related categories to reduce the ambiguity in the annotation process. The 13 meta categories are *bag*, *belt*, *boots*, *footwear*, *outer*, *dress*, *sunglasses*, *pants*, *top*, *shorts*, *skirt*, *headwear*, *scarf&tie*. The detailed mapping from the original labels to the meta categories is shown in Table 2. Some examples of original images, pixel-level segmentation masks, and bounding boxes are shown in Figure 1. We also visualize the distribution of the clothing categories in this dataset in Figure 2. The most common objects in this dataset are *footwear*, *top*, *outer*, *pants*, and *bags*. Most images contain 3 to 5 fashion objects. We also see that categories such as *belts*, *headwear*, and *scarf&tie* account for a small portion of the outfit, while *dress*, *outer*, *pants* and *skirts* fall on the large side of the instance size spectrum. Since the ModaNet dataset was annotated using polygons, we present the statistics of polygon annotations in Figure 3. We can see that categories such as *outer*, *dress*, *boots* and *pants* require the most number of clicks to annotate due to their size and shape, while *sunglasses* and *belts* have the least number of vertices in their polygons. Additionally, a clothing instance can have a lot of details, e.g., straps on heels or it can be occluded by body parts or other clothing layers, hence requiring multiple polygons to annotate it fully. We see that *footwear*, *outer* and *boots* require the most number of polygon segments, while *sunglasses* and *belts* are captured in one polygon. Finally, we observe that with the size of instances growing, the number of vertices increases correspondingly, with *belts* and *sunglasses* as exceptions hinting at their less complex shape characteristics.

Table 1: Comparison of ModaNet with other datasets for fashion parsing. ModaNet surpasses previous datasets in terms of annotation granularity and scale. \checkmark^* indicates the annotations are not included in the original dataset. The count of categories excludes non-fashion categories, such as *hair*, *skin*, *face*, *background* and *null*.

	DeepFashion [30]	CFPD [26]	CCP [42]	Fashionista [41]	HPW[20]	ModaNet
# of images	800,000	2,682	1,004	685	1,833	55,176
# of categories	50	19	56	53	11	13
Pixel annotation	\times	\checkmark	\checkmark	\checkmark	\checkmark	\checkmark
Bounding box	landmarks	\checkmark^*	\checkmark^*	\checkmark^*	\checkmark^*	\checkmark
Polygon	\times	\times	\times	\times	\times	\checkmark



Figure 1: Examples of original images with corresponding pixel-level segmentation masks and bounding box annotations of the proposed ModaNet dataset. The first row shows the original color street image containing a person with fashion products. The second row indicates the pixel-wise annotation for the fashion product, where color is encoded to represent the fashion product category. The third row represents the bounding box annotation overlaying on the color images. Best view in color.

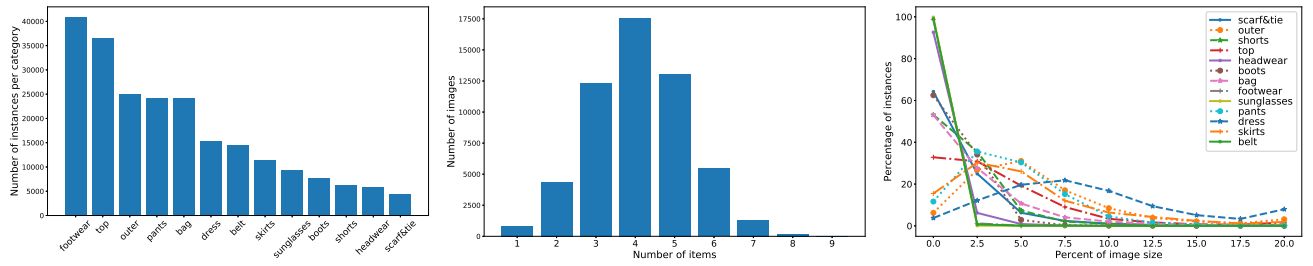


Figure 2: Dataset statistics. Left: the number of instances for each clothing category in descending order. Middle: the distribution of images from minimum number of annotated items per image to the maximum number of items per image. We can see that on average most images contain four annotated items. Right: The distribution of instance sizes across categories in ModaNet dataset. Best viewed in color.

4 MODANET APPLICATIONS

4.1 Object Detection for Fashion

The dataset enables fashion item detection, where each fashion item is localized and assigned with a category label, which can be further used for visual search and product recommendation.

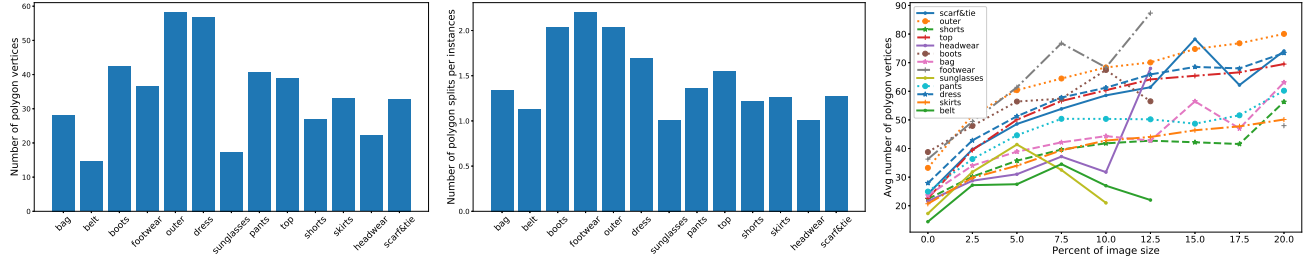


Figure 3: Annotation polygon statistics. Left: average number of vertices in polygon annotations for each category. Middle: average number of segments in polygon annotations of an instance of each category. Right: total number of vertices in the annotation polygons for each instance vs the size of the instance. Best viewed in color.

Table 2: ModaNet statistics. We group highly-related categories to form 13 meta categories.

Meta	Raw	#Train	#Val	Avg Inst. size
bag	bag	36, 699	2, 155	4.88%
belt	belt	13, 743	771	0.46%
boots	boots	7, 068	691	2.40%
footwear	footwear	39, 364	1, 617	0.96%
outer	coat, jacket, suit, blazers	23, 743	1, 358	7.48%
dress	dress, t-shirt dress	14, 460	804	10.49%
sunglasses	sunglasses	8, 780	524	0.31%
pants	pants, jeans, leggings	23, 075	1, 172	5.65%
top	top, blouse, t-shirt, shirt	34, 745	1, 862	4.83%
shorts	shorts	5, 775	429	2.86%
skirt	skirt	10, 860	555	6.40%
headwear	headwear	5, 405	491	1.25%
scarf&tie	scarf, tie	3, 990	378	2.55%

4.1.1 Groundtruth generation. Given pixel-level and polygon annotations, we can easily infer bounding boxes for training images. In this work, we choose to generate bounding boxes from the polygon annotations as the boundary information is easily accessible. While a single fashion item might be annotated by multiple polygons due to composition, pose variation and occlusion in some cases, we assume that there is only one person and each fashion item only appears once (twice for a pair of shoes) and merge them to ensure a single bounding box. Also, we discard all boxes with the size smaller than 100 pixels to ensure the training data is large enough to train a reasonable model. We split the whole dataset into training containing 52, 377 images and a validation set containing the remaining 2, 799 images. The split enforces that each category from the validation set contains at least 500 instances so that the validation accuracy is reliable. Note that it is not feasible to enforce that the number of instances in the validation set for each category is precisely proportional to the total number of instances in the dataset due to that multiple items appear in a single image. All of our subsequent experiments follow the same training and validation split. Some example annotations are shown in Figure 1. All the bounding box annotations will be made available along with the dataset.

4.1.2 Detectors. While there are numerous object detectors available in the literature, we choose three most popular detectors to evaluate their performance on the dataset, which are Faster RCNN [32], SSD [28] and YOLO [31]. Both SSD and YOLO are real-time detectors and have similar network architectures, which can be used for mobile devices. We compare their performance to investigate the trade-off between accuracy and efficiency. Faster RCNN is more accurate but takes more time during inference, making it more suitable for offline applications. Specifically, for Faster RCNN, the backbone network is Inception-ResNet [39]. We use Inception V2 network [39] for SSD and YOLO v2 network for YOLO detector.

4.1.3 Performance comparison. We evaluate and compare the performance of Faster RCNN, SSD and YOLO on our ModaNet dataset using mean average precision (mAP) as the evaluation metric. Meanwhile, we also show the average precision (AP) per category to understand which categories are more challenging to the detectors. Also, we adjust the IOU threshold and compute mAP based on varying IOU thresholds to provide more insights of how well the predicted bounding boxes align with the ground truth as a robustness measurement.

In Figure 4, we show the precision-recall curve per category of each detector with the IOU threshold 0.5. Apparently, the Faster RCNN detector achieves the best overall accuracy and on all categories, which aligns well with our expectation. Specifically, all the detectors do not perform well on *scarf&tie* category while all achieve promising results (with mAP over 0.9) on the *pants*, *headwear* and *sunglasses* categories. Since there are abundant samples of pants in various poses, and sunglasses and headwear are usually of rigid shape without occlusion, it is easier for the model to recognize and localize these instances from street photos. In contrast, scarves and ties are highly deformable and often occluded by human bodies or other clothes, adding great difficulty to model training. Qualitative comparisons of the three detectors are presented in Figure 5.

To evaluate the robustness of these detectors against varying IOU threshold, we increase the threshold from 0.5 to 0.9 by 0.1 increment and calculate mAP regarding to each IOU threshold. The results are shown in Figure 6. As expected, the mAP and AP per category decreases as more rigorous criterion is applied. We find that the detectors are relatively robust for categories such as *pants* and *headwear* as the AP only slightly drops, remaining over 0.8 even though the IOU threshold is as high as 0.8. It shows

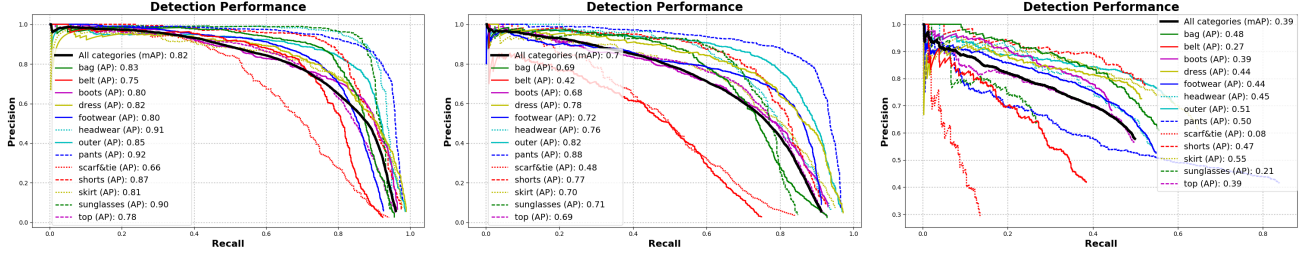


Figure 4: Performance comparison of Faster RCNN (left), SSD (middle) and YOLO (right). Best view in color.

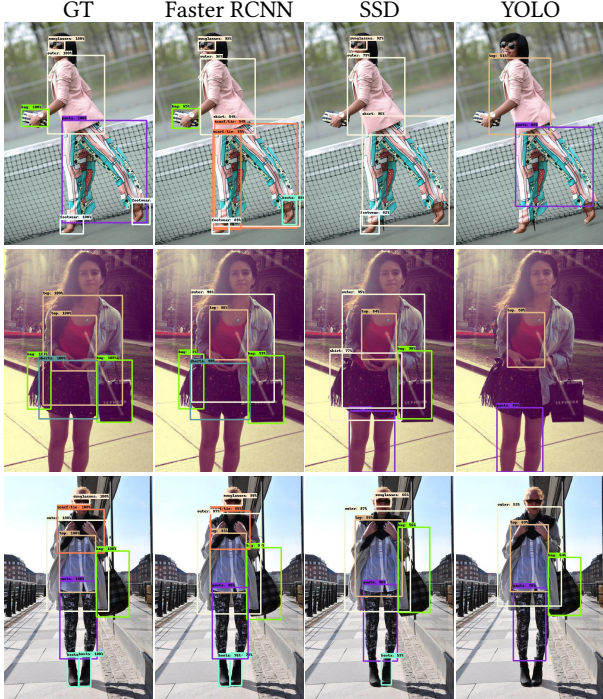


Figure 5: Qualitative comparisons of Faster RCNN, SSD and YOLO.

that these categories are easier to handle. In contrast, categories of small and deformable objects like *sunglasses*, *belt* and *scarf&tie* are more difficult for the detectors. A stand-out example is *sunglasses* category, on which the Faster RCNN achieves the second best AP when $\text{IOU}=0.5$. However, when we increase the IOU threshold, the corresponding AP dramatically drops to the worst when $\text{IOU}=0.9$. Such case implies that the detected bounding boxes do not have a high overlap ratio with the groundtruth. Therefore, more effort should be put into developing detectors that can better handle small and highly deformable objects for fashion.

4.2 Semantic Segmentation for Fashion

ModaNet dataset provides pixel-wise annotation to enable semantic segmentation research for fashion.

4.2.1 Groundtruth generation. Given the polygon annotations, we generate pixel-wise annotations. For the polygon annotations that cover a single object, it is straightforward to obtain the corresponding pixel-wise annotations. In other cases, the same object might be occluded and there are multiple polygon annotations to cover the same object. In the human annotations, this information is included and the multiple polygon annotations of the same object are grouped together. For objects like shoes, we assign the same semantic labels to the both left and right shoes as long as they are visible. We follow the same training/validation split as fashion item detection, so that we have 52,377 images in the training set and 2,799 images in the validation set.

4.2.2 Approaches. Semantic segmentation is a popular research direction. Many of the semantic segmentation approaches are developed to tackle generic things and stuff from images. We evaluate several most representative approaches on ModaNet and provide the baseline results to motivate future research. These approaches are: FCNs [34]¹, CRFasRNN [46]² and DeepLabv3+ [5]³. DeepLab [4] is a state-of-the-art semantic image segmentation approach on the PASCAL VOC dataset. It has been improved by using atrous convolution, multi-scale training, and various base models including VGG, ResNet-101 and Xception. In order to measure the performance of different approaches, we adapt the standard mean pixel intersection-over-union (IOU), with the mean taken over all classes, as well as precision, recall, and F-1 scores.

For FCN-32 [34], FCN-8 [34], and CRFasRNN [46], we follow the pipeline in Caffe from the original authors. We adapt the base model of VGG [38] network with batch normalization [37], which has obtained 26.9% top-1 error on the ImageNet-2012 semantic segmentation task. We train those models using batch size 1, base learning rate 1×10^{-9} , learning rate decay step 52,378, step learning strategy, and stochastic gradient descent optimization method. We use the default set of initial parameters of CRFasRNN for PASCAL VOC dataset. We For FCN, we conduct experiments using Caffe, and evaluate its performance (using original VGG network) using Pytorch.

For DeepLabv3+ [5], we take the public available TensorFlow implementation and ImageNet pre-trained Xception-65 model [6], and fine-tune on the ModaNet dataset for 115 epochs using batch size 6, base learning rate 5×10^{-4} , learning rate decay step 52,378,

¹<https://github.com/shelhamer/fcn.berkeleyvision.org>

²<https://github.com/torrvision/crfasrn>

³<https://github.com/tensorflow/models/tree/master/research/deeplab>

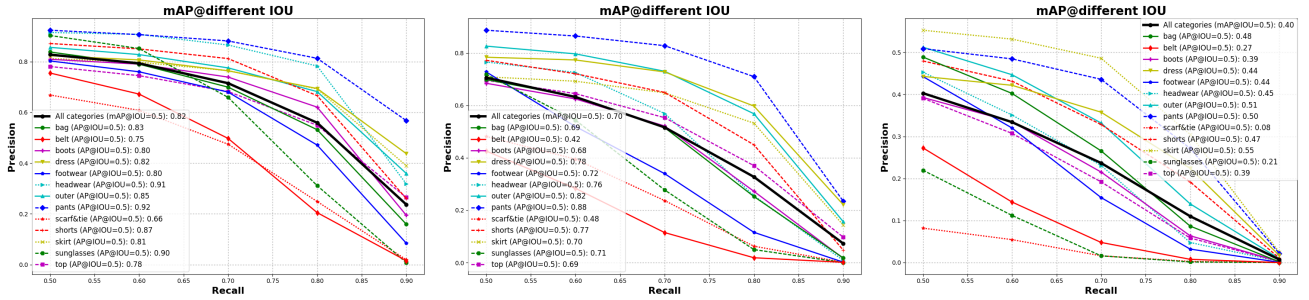


Figure 6: Performance comparison of Faster RCNN (left), SSD (middle) and YOLO (right). Best view in color.

step learning strategy and stochastic gradient descent optimization method. The base model Xception-65 has obtained 21.0% top-1 error on the ImageNet-2012 semantic segmentation task.

4.2.3 Performance comparison. We find that DeepLabV3+ performs significantly better than the alternative approaches across all metrics, which is consistent with the results on PASCAL VOC leaderboard. As shown in Table 3, Table 4, Table 5, and Table 6, CRFasRNN improves performance for categories with large extend, while slightly decreases the performance for categories with smaller extend. Since the bilateral filter in CRFasRNN uses the same set of parameters for all categories, CRFasRNN tends to over-smooth out small objects, such as objects from *sunglasses* category, thus leads to poorer performance. CRFasRNN maintains better shape of some objects like *outer* and *pants*, since these fashion objects are often color consistent. In Figure 7, we also present F-1 scores, which confirm with our observations.

4.3 Polygon Prediction for Fashion

Recognizing clothing design and detecting polygon keypoints of fashion items are useful in fashion applications. Polygon is another typical form of annotations in semantic segmentation, apart from pixel-level segmentation masks. It is considered to be more accurate than the alternatives such as superpixel-based annotations, although manually annotating images using polygons is time-expensive. In this work, given high-quality polygons from human annotators, we conduct experiments to predict polygons for individual fashion items given an input image.

4.3.1 Approaches. Recent approaches such as PolygonRNN [3] and Polygon-RNN++ [1] have addressed the problem of polygon prediction directly using neural networks. We set up the baseline performance on ModaNet using the pre-trained model of Polygon-RNN++. This model is an encoder-decoder network. The encoder produces image features that are used to predict the first vertex, and then the first vertex and the image features are fed to the recurrent decoder. The recurrent neural network exploits the visual attention at each time step to produce polygon vertices. A learned evaluator is employed to select the best polygon from a set of candidates proposed by the decoder. In the final stage, a graph-based neural network re-adjusts the polygons and augments them with additional vertices at a higher resolution. The base model in

the encoder is a modified ResNet-50, which has reduced stride and dilation factors.

4.3.2 Performance. In our experiment, we adapt the public available Polygon-RNN++ model that is pre-trained on the Cityscape dataset to produce the baseline performance. We form the inputs of Polygon-RNN++ using the cropped images based on the Faster-RCNN detection results. The polygon predictions of polygon-RNN++ are evaluated on the validation set of ModaNet dataset. We convert the polygon predictions to the mask-like predictions. A perfect polygon prediction should give the same semantic image segmentation mask created by human annotators. Using the masks for semantic segmentation as groundtruth, we evaluate how well the results from the pre-trained polygon-RNN++ model align well with the segmentation masks. The Polygon-RNN++ model achieves mean IOU 30.7%, mean precision 83.4%, mean recall 32.5% and mean F-1 score 45.0%. We hope such preliminary baseline results on the ModaNet dataset would motivate future research on polygon prediction.

4.4 Color Attribute Prediction Prototype

One application of semantic segmentation is to predict the color attribute name given a fashion product. We develop such a prototype based on ModaNet dataset. We first conduct the semantic image segmentation, and then predict the color attribute names by mapping the mean RGB values for each segment to a fine-grained color name space⁴. The example results are presented in Figure 8. The image and the predicted masks are shown on the left, and the predicted text including the color attribute names and the fashion object category names is shown on the right.

5 CONCLUSIONS

In this work, we introduce a new large-scale image dataset with polygon annotations that help develop vision algorithms for fashion. The dataset contains street fashion photos that exhibit various challenges, such as human poses, lighting, occlusion, deformation, etc., which well captures the scenarios in the real world. Different types of annotations are provided including polygons, pixel-level segmentation masks, and bounding boxes. We have conducted experiments on fashion object detection, semantic segmentation, and polygon predictions. We also demonstrate that the proposed dataset is suitable for training models to achieve promising application such

⁴<https://github.com/ayushoriginal/Optimized-RGB-To-ColorName>

Figure 7: F-1 scores by category.

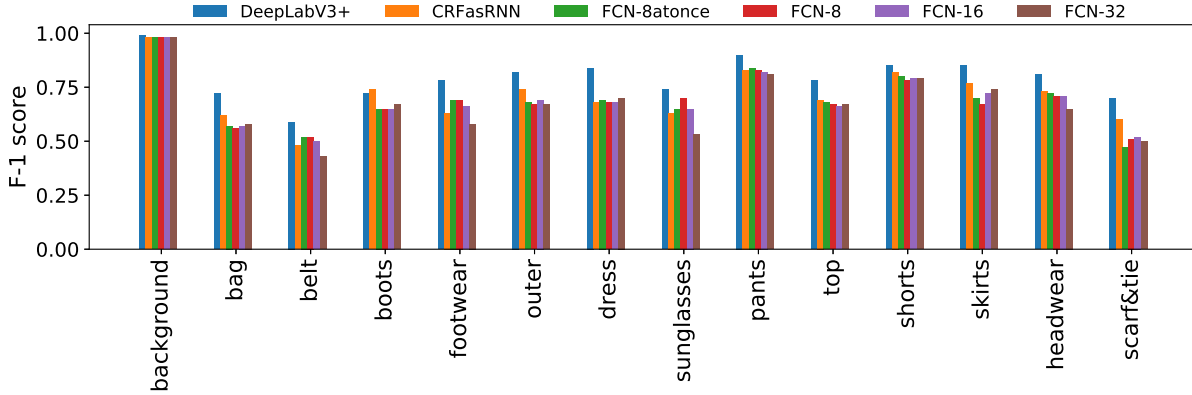


Table 3: IoU per class.

Method	background	bag	belt	boots	footwear	outer	dress	sunglasses	pants	top	shorts	skirts	headwear	scarf&tie
FCN-32 [34]	0.95	0.27	0.12	0.32	0.33	0.36	0.28	0.25	0.51	0.38	0.40	0.28	0.33	0.17
FCN-16 [34]	0.96	0.26	0.19	0.32	0.38	0.35	0.25	0.37	0.51	0.38	0.40	0.23	0.41	0.16
FCN-8 [34]	0.96	0.24	0.21	0.32	0.40	0.35	0.28	0.41	0.51	0.38	0.40	0.24	0.44	0.18
FCN-8atonce [34]	0.96	0.26	0.20	0.31	0.40	0.35	0.29	0.36	0.50	0.39	0.38	0.26	0.44	0.16
CRFasRNN [46]	0.96	0.30	0.18	0.41	0.39	0.43	0.32	0.36	0.56	0.40	0.44	0.26	0.45	0.22
DeepLabV3+ [5]	0.98	0.42	0.28	0.40	0.51	0.56	0.52	0.46	0.68	0.55	0.53	0.41	0.55	0.31

Table 4: Precision per class.

Method	background	bag	belt	boots	footwear	outer	dress	sunglasses	pants	top	shorts	skirts	headwear	scarf&tie
FCN-32 [34]	0.97	0.52	0.37	0.59	0.51	0.53	0.44	0.53	0.60	0.53	0.56	0.45	0.47	0.46
FCN-16 [34]	0.97	0.52	0.42	0.64	0.58	0.47	0.38	0.66	0.64	0.59	0.58	0.35	0.65	0.36
FCN-8 [34]	0.97	0.42	0.51	0.66	0.58	0.52	0.46	0.74	0.61	0.49	0.62	0.45	0.74	0.53
FCN-8atonce [34]	0.97	0.51	0.43	0.75	0.59	0.52	0.45	0.74	0.59	0.52	0.51	0.44	0.72	0.55
CRFasRNN [46]	0.96	0.49	0.57	0.66	0.68	0.58	0.58	0.65	0.76	0.61	0.61	0.37	0.73	0.44
DeepLabV3+ [5]	0.99	0.62	0.53	0.75	0.62	0.70	0.67	0.74	0.75	0.69	0.69	0.56	0.74	0.51

Table 5: Recall per class.

Method	background	bag	belt	boots	footwear	outer	dress	sunglasses	pants	top	shorts	skirts	headwear	scarf&tie
FCN-32 [34]	0.98	0.43	0.23	0.48	0.53	0.62	0.60	0.44	0.81	0.63	0.66	0.53	0.67	0.31
FCN-16 [34]	0.98	0.42	0.37	0.47	0.60	0.69	0.61	0.54	0.78	0.57	0.64	0.59	0.62	0.36
FCN-8 [34]	0.99	0.47	0.37	0.44	0.64	0.63	0.57	0.53	0.81	0.71	0.61	0.47	0.57	0.28
FCN-8atonce [34]	0.99	0.42	0.38	0.39	0.63	0.63	0.58	0.48	0.83	0.68	0.69	0.51	0.59	0.24
CRFasRNN [46]	0.99	0.53	0.26	0.59	0.52	0.70	0.50	0.54	0.71	0.58	0.66	0.62	0.60	0.41
DeepLabV3+ [5]	0.99	0.61	0.48	0.50	0.78	0.78	0.73	0.60	0.88	0.74	0.74	0.69	0.72	0.54

as color attribute prediction. We release this dataset to facilitate future computer vision research on fashion understanding.

REFERENCES

- [1] David Acuna, Huan Ling, Amlan Kar, and Sanja Fidler. 2018. Efficient Interactive Annotation of Segmentation Datasets with Polygon-RNN++. In *CVPR*.
- [2] Navaneeth Bodla, Bharat Singh, Rama Chellappa, and Larry S. Davis. 2017. Soft-NMS - Improving Object Detection with One Line of Code. In *ICCV*. 5562–5570.
- [3] Lluis Castrejon, Kaustav Kundu, Raquel Urtasun, and Sanja Fidler. 2017. Annotating Object Instances with a Polygon-RNN. In *CVPR*.
- [4] Liang-Chieh Chen, George Papandreou, Iasonas Kokkinos, Kevin Murphy, and Alan L. Yuille. 2018. DeepLab: Semantic Image Segmentation with Deep Convolutional Nets, Atrous Convolution, and Fully Connected CRFs. *IEEE Trans. Pattern Anal. Mach. Intell.* 40 (2018), 834–848, Issue 4.
- [5] Liang-Chieh Chen, Yukun Zhu, George Papandreou, Florian Schroff, and Hartwig Adam. 2018. Encoder-Decoder with Atrous Separable Convolution for Semantic Image Segmentation. In *CVPR*.
- [6] Francois Chollet. 2017. Xception: Deep Learning with Depthwise Separable Convolutions. In *CVPR*.
- [7] Jifeng Dai, Yi Li, Kaiming He, and Jian Sun. 2016. R-FCN: Object Detection via Region-based Fully Convolutional Networks. In *NIPS*.
- [8] Jifeng Dai, Haozhi Qi, Yuwen Xiong, Yi Li, Guodong Zhang, Han Hu, and Yichen Wei. 2017. Deformable Convolutional Networks. In *ICCV*. 764–773.

Table 6: F-1 score per class.

Method	background	bag	belt	boots	footwear	outer	dress	sunglasses	pants	top	shorts	skirts	headwear	scarf&tie
FCN-32 [34]	0.98	0.58	0.43	0.67	0.58	0.67	0.70	0.53	0.81	0.67	0.79	0.74	0.65	0.50
FCN-16 [34]	0.98	0.57	0.50	0.65	0.66	0.69	0.68	0.65	0.82	0.66	0.79	0.72	0.71	0.52
FCN-8 [34]	0.98	0.56	0.52	0.65	0.69	0.67	0.68	0.70	0.83	0.67	0.78	0.67	0.71	0.51
FCN-8satonce [34]	0.98	0.57	0.52	0.65	0.69	0.68	0.69	0.65	0.84	0.68	0.80	0.70	0.72	0.47
CRFasRNN [46]	0.98	0.62	0.48	0.74	0.63	0.74	0.68	0.63	0.83	0.69	0.82	0.77	0.73	0.60
DeepLabV3+ [5]	0.99	0.72	0.59	0.72	0.78	0.82	0.84	0.74	0.90	0.78	0.85	0.85	0.81	0.70



Figure 8: Color attribute prediction using semantic image segmentation. The color names are printed with the predicted mean RGB values for the corresponding category. Best viewed in color.

[9] Jia Deng, Wei Dong, Richard Socher, Li-Jia Li, Kai Li, and Li Fei-Fei. 2009. Imagenet: A large-scale hierarchical image database. In *CVPR*.

[10] Jian Dong, Qiang Chen, Wei Xia, Zhongyang Huang, and Shuicheng Yan. 2013. A deformable mixture parsing model with parselets. In *ICCV*.

[11] Ross B. Girshick. 2015. Fast R-CNN. In *ICCV*. 1440–1448.

[12] Ross B. Girshick, Jeff Donahue, Trevor Darrell, and Jitendra Malik. 2014. Rich Feature Hierarchies for Accurate Object Detection and Semantic Segmentation. In *CVPR*. 580–587.

[13] Kota Hara, Vignesh Jagadeesh, and Robinson Piramuthu. 2016. Fashion apparel detection: The role of deep convolutional neural network and pose-dependent priors. In *WACV*. 1–9.

[14] Bharath Hariharan, Pablo Arbelaez, Ross Girshick, and Jitendra Malik. 2014. Simultaneous Detection and Segmentation. In *CVCC*.

[15] Kaiming He, Xiangyu Zhang, Shaoqing Ren, and Jian Sun. 2016. Deep Residual Learning for Image Recognition.

[16] Xuming He, Richard S Zemel, and Miguel A Carreira-Perpinan. 2014. Multiscale Conditional Random Fields for Image Labeling. In *CVPR*.

[17] Junshi Huang, Rogério Schmidt Feris, Qiang Chen, and Shuicheng Yan. 2015. Cross-Domain Image Retrieval with a Dual Attribute-Aware Ranking Network. In *ICCV*. 1062–1070.

[18] M. Hadi Kiapour, Xufeng Han, Svetlana Lazebnik, Alexander C. Berg, and Tamara L. Berg. 2015. Where to Buy It: Matching Street Clothing Photos in Online Shops. In *ICCV*. 3343–3351.

[19] Lubor Ladicky, Chris Russell, Pushmeet Kohli, and Philip HS Torr. 2009. Associative hierarchical crfs for object class image segmentation. In *ICCV*.

[20] Xiaodan Liang, Si Liu, Xiaohui Shen, Jianchao Yang, Luoqi Liu, Jian Dong, Liang Lin, and Shuicheng Yan. 2015. Deep Human Parsing with Active Template Regression. *IEEE Trans. Pattern Anal. Mach. Intell.* 37, 12 (2015), 2402–2414.

[21] Xiaodan Liang, Chunyan Xu, Xiaohui Shen, Jianchao Yang, Si Liu, Jinhui Tang, Liang Lin, and Shuicheng Yan. 2015. Human Parsing with Contextualized Convolutional Neural Network. In *ICCV*.

[22] G. Lin, C. Shen, A. van den Hengel, and I. D. Reid. 2017. Exploring context with deep structured models for semantic segmentation. In *CVPR*.

[23] Tsung-Yi Lin, Piotr Dollár, Ross B. Girshick, Kaiming He, Bharath Hariharan, and Serge J. Belongie. 2017. Feature Pyramid Networks for Object Detection. In *CVPR*. 936–944.

[24] Tsung-Yi Lin, Priya Goyal, Ross B. Girshick, Kaiming He, and Piotr Dollár. 2017. Focal Loss for Dense Object Detection. In *ICCV*. 2999–3007.

[25] Tsung-Yi Lin, Michael Maire, Serge Belongie, James Hays, Pietro Perona, Deva Ramanan, Piotr Dollar, and C Lawrence Zitnick. 2014. Microsoft coco: Common objects in context. In *ECCV*.

[26] Si Liu, Jiashi Feng, Csaba Domokos, Hui Xu, Junshi Huang, Zhenzhen Hu, and Shuicheng Yan. 2014. Fashion Parsing With Weak Color-Category Labels. *IEEE Trans. Multimedia* 16, 1 (2014), 253–265.

[27] Si Liu, Xiaodan Liang, Luoqi Liu, Ke Lu, Liang Lin, and Shuicheng Yan. 2014. Fashion Parsing with Video Context. In *ACM MultiMedia*.

[28] Wei Liu, Dragomir Anguelov, Dumitru Erhan, Christian Szegedy, Scott Reed, Cheng-Yang Fu, and Alexander C. Berg. 2016. SSD: Single Shot MultiBox Detector. In *ECCV*.

[29] Ziwei Liu, X. Li, P. Luo, C.-C. Loy, and X. Tang. 2017. Deep learning markov random field for semantic segmentation. *IEEE Trans. Pattern Anal. Mach. Intell.* 35, 1 (2017), 37–52.

[30] Ziwei Liu, Ping Luo, Shi Qiu, Xiaogang Wang, and Xiaou Tang. 2016. DeepFashion: Powering Robust Clothes Recognition and Retrieval with Rich Annotations. In *CVPR*. 1096–1104.

[31] Joseph Redmon, Santosh Divvala, Ross Girshick, and Ali Farhadi. 2016. You only look once: Unified, real-time object detection. In *CVPR*.

[32] Shaoqing Ren, Kaiming He, Ross Girshick, and Jian Sun. 2015. Faster R-CNN: Towards Real-Time Object Detection with Region Proposal Networks. In *NIPS*.

[33] A. G. Schwing and R. Urtasun. 2015. Fully connected deep structured networks. In *arXiv:1503.02351*.

[34] Evan Shelhamer, Jonathon Long, and Trevor Darrell. 2016. Fully Convolutional Networks for Semantic Segmentation. *IEEE Trans. Pattern Anal. Mach. Intell.* 39 (2016), 640–651. Issue 4.

[35] Jamie Shotton, John Winn, Carsten Rother, and Antonio Criminisi. 2006. Textronboot: Joint appearance, shape and context modeling for multi-class object recognition and segmentation. In *ECCV*.

[36] Abhinav Shrivastava, Abhinav Gupta, and Ross B. Girshick. 2016. Training Region-Based Object Detectors with Online Hard Example Mining. In *CVPR*. 761–769.

[37] Marcel Simon, Erik Rodner, and Joachim Denzler. 2016. ImageNet pre-trained models with batch normalization. *arXiv preprint arXiv:1612.01452* (2016).

[38] K. Simonyan and A. Zisserman. 2015. Very Deep Convolutional Networks for Large-Scale Image Recognition. In *ICLR*.

[39] Christian Szegedy, Sergey Ioffe, Vincent Vanhoucke, and Alexander A Alemi. 2017. Inception-v4, inception-resnet and the impact of residual connections on learning. In *AAAI*.

[40] Kota Yamaguchi, M. Hadi Kiapour, and Tamara L. Berg. 2013. Paper Doll Parsing: Retrieving Similar Styles to Parse Clothing Items. In *ICCV*. 3519–3526.

[41] Kota Yamaguchi, M. Hadi Kiapour, Luis E. Ortiz, and Tamara L. Berg. 2012. Parsing clothing in fashion photographs. In *CVPR*. 3570–3577.

[42] Wei Yang, Ping Luo, and Liang Lin. 2014. Clothing Co-parsing by Joint Image Segmentation and Labeling. In *CVPR*. 3182–3189.

[43] Aron Yu and Kristen Grauman. 2014. Fine-Grained Visual Comparisons with Local Learning. In *CVPR*. 192–199.

[44] Fisher Yu and Vladlen Koltun. 2016. Multi-Scale Context Aggregation by Dilated Convolutions. In *ICLR*.

[45] HengShuang Zhao, Jianping Shi, Xiaojuan Qi, Xiaogang Wang, and Jiaya Jia. 2017. Pyramid Scene Parsing Network. In *CVPR*. 1063–6919.

[46] Shuai Zheng, Sadeep Jayasumana, Bernardino Romera-Paredes, Vibhav Vineet, Zhizhong Su, Dalong Du, Chang Huang, and Philip H. S. Torr. 2015. Conditional Random Fields as Recurrent Neural Networks. In *ICCV*. 1529–1537.